Proceedings of ERAD 2006

Simulation of the specific differential phase (K_{DP}) from 2D-Video-Distrometer measurements at S- and C-band wavelengths

Franz Teschl[1], Walter L. Randeu[1,2], Michael Schönhuber[2], Reinhard Teschl[1]

[1] Department of Broadband Communications, Graz University of Technology, Graz (Austria).

[2] Institute of Applied Systems Technology Joanneum Research, Graz (Austria).

1 Introduction

For estimating rainrates (R) from radar measurements, the specific differential phase (K_{DP}) has several advantages over the radar reflectivity factor (Z). K_{DP} is for instance unsusceptible to the radar calibration error, partial beam blockage, and attenuation. R-K_{DP} relationships are therefore especially useful to overcome the problem of attenuation of C-band radar waves in heavy rainfall. A variety of physical and empirical approaches exists to find $R(K_{DP})$ estimators, resulting in a wide range of relationships (Table 1). At C-band the situation is more complex since the influence of the raindrop temperature is not negligibly small as opposed to S-band.

Table 1. R-K_{DP} relationships for S-band. (K_{DP} units are ° km^{-1}; R is in mm h^{-1})

Study	R-K_{DP} relationship
Aydin and Giridhar (1992)	
$1.5 < K_{DP} < 7$° km^{-1}:	$R = 33.77\ K_{DP}^{0.97}$
$0.01 < K_{DP} < 1.5$° km^{-1}:	$R = 36.15\ K_{DP}^{0.84}$
Sachidananda and Zrnić (1987)	$R = 40.56\ K_{DP}^{0.866}$
Jameson (1991)	$R = 41.46\ K_{DP}^{0.838}$
Illingworth and Blackman (2002)	$R = 50.10\ K_{DP}^{0.7}$
Bringi and Chandrasekhar (2001)	$R = 50.70\ K_{DP}^{0.866}$

In the present study K_{DP} was calculated for hundreds of rain events, observed with a 2D-Video-Distrometer (Schönhuber et al., 1994), in the mountains of Styria, Austria. Relationships in the form $R = a\ K_{DP}^{b}$ were established for S- and C-band. The influence of temperature, the canting angle of the raindrops, the elevation angle of the radar antenna, and the effect of different shape models on K_{DP} are shown, and it is discussed if these parameters can account for the variety of R-K_{DP} relationships.

Correspondence to: Franz Teschl.

franz.teschl@tugraz.at

2 Data

The raindrop-size distribution measurements were obtained from a 2D-Video-Distrometer positioned at Mt. Präbichl in the Province of Styria, Austria. The analyzed data were recorded during convective and stratiform rainfall events in the years 2000 and 2001. The drop-size distribution was discretized in 0.25 mm steps for the equivolumetric sphere diameter D and averages over 1 minute have been considered.

3 Methodology

The one-way specific differential phase K_{DP} was computed from the drop size distribution with (Oguchi, 1983)

$$K_{DP} = \left(180 \cdot 10^3\right)\frac{\lambda}{\pi} \cdot Re \int_0^{D_{max}} \left[f_{hh}(D) - f_{vv}(D)\right] \cdot N(D) dD \qquad (1)$$

where

λ wavelength (m)

$N(D)$ drop-size distribution (mm^{-1} m^{-3})

D drop diameter (mm)

D_{max} maximum drop diameter (mm)

Re refers to the real part of the integral

f_{hh} and f_{vv} are the forward-scattering amplitudes for horizontally and vertically polarized waves (in meters).

Conventionally the units of K_{DP} are ° km^{-1}.

The forward-scattering amplitudes of single raindrops were calculated by a point matching algorithm applying raindrop shapes according to the model of Pruppacher and Beard (1970). The effect of other raindrop-shape models is compared in section 6.

The forward-scattering amplitudes were calculated for 10° C raindrop temperature. The effect of temperatures between 0 and 30° C is discussed in section 5. The complex relative dielectric permittivity ε of water was determined according to Ray (1972).

The calculations were carried out at S-band (2.8 GHz/10.7 cm) and C-band (5.625 GHz/5.3 cm wavelength). For comparison also results at X-band (9.6 GHz/3.1 cm) are presented.

4 Results

Figures 1 and 2 show scatterplots of R versus K_{DP} for S- and C-band.

The relationships found at 10° C from a least square fit of log R and log K_{DP} over 249 observed drop-size distributions are

$$R = 35.33\ K_{DP}^{0.842} \quad (2)$$

for S-band,

$$R = 18.87\ K_{DP}^{0.835} \quad (3)$$

for C-band, and

$$R = 11.84\ K_{DP}^{0.836} \quad (4)$$

for X-band.

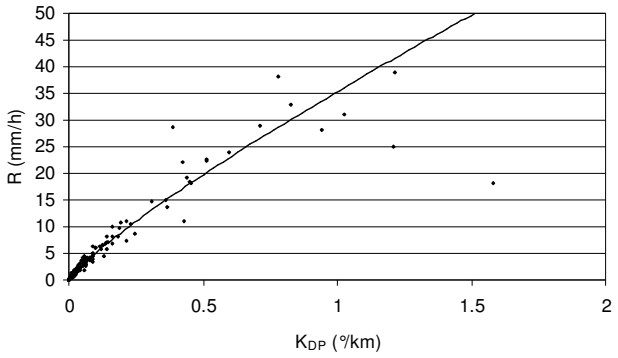

Fig. 1. Scatterplot of R versus K_{DP} at S-band (10.7 cm wavelength) and 10° C raindrop temperature. The solid curve corresponds to (2).

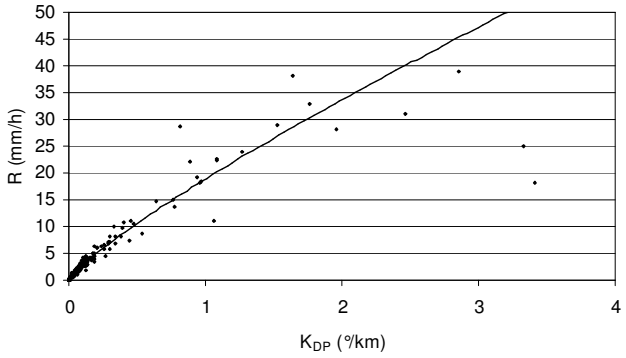

Fig. 2. Scatterplot of R versus K_{DP} at C-band (5.3 cm wavelength) and 10° C raindrop temperature. The solid curve corresponds to (3).

5 Effect of raindrop temperature on K_{DP}

For a given wavelength and drop-size distribution, K_{DP} alters with the real part of the forward-scattering amplitudes of the raindrops (1). The forward-scattering amplitudes of raindrops depend besides their shapes also on the dielectric properties of the water and as a consequence on the temperature. Thus, below the difference between the real parts of horizontal and vertical forward scattering amplitude $Re(f_{hh} - f_{vv})$ are plotted versus equivolumetric sphere diameter for different wavelengths.

At S-band, effects of temperature on K_{DP} are negligibly small. Fig. 3 shows $Re(f_{hh} - f_{vv})$ at 10.7 cm wavelength and 10° C. For all raindrop temperatures considered, the curve is equal.

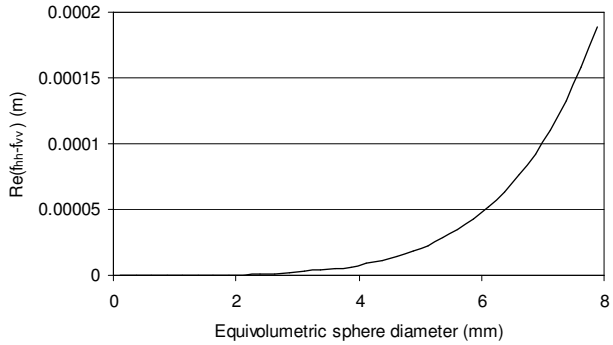

Fig 3. Difference between the real parts of horizontal and vertical forward scattering amplitude $Re(f_{hh} - f_{vv})$ versus equivolumetric sphere diameter of the raindrop, at 10.7 cm wavelength.

At C-band, effects of temperature on K_{DP} are no longer negligible. Fig. 4 shows the situation for 0, 10, 20 and 30° C.

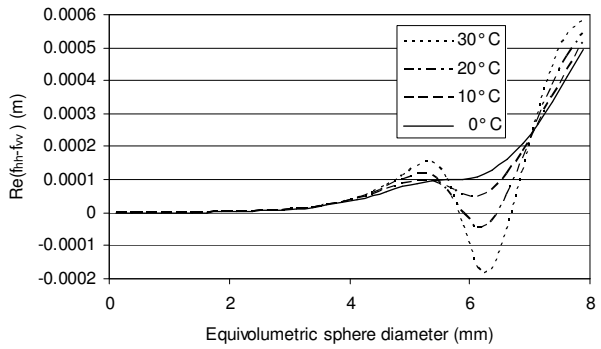

Fig. 4. Difference between the real parts of horizontal and vertical forward scattering amplitude $Re(f_{hh} - f_{vv})$ versus equivolumetric sphere diameter of the raindrop, at 5.3 cm wavelength and temperatures between 0 and 30° C.

For equivolumetric sphere diameters up to 4 mm the temperature has no effect, while for bigger ones the effect can be significant. E. g. for 6 mm raindrops $Re(f_{hh} - f_{vv})$ turns negative at 20° C. This means that K_{DP} for a volume containing 6 mm drops can be less than the same volume without these drops. It seems that resonance effects which make the use of Z_{DR} ambiguous at C-band frequency and around 6 mm drop diameter, affect also K_{DP} in an adverse way. However, practical significance of this effect would

only be strong for monodisperse drop spectra. Since in the analyzed distrometer data, 6 mm raindrops occurred sporadically, no significant variation in the R-K_{DP} relationship was observed at higher temperatures.

At X-band the effect of the temperature is rather small as shown in Fig. 5. The "resonance" region now resides just below 4 mm drop diameter, but is not very pronounced.

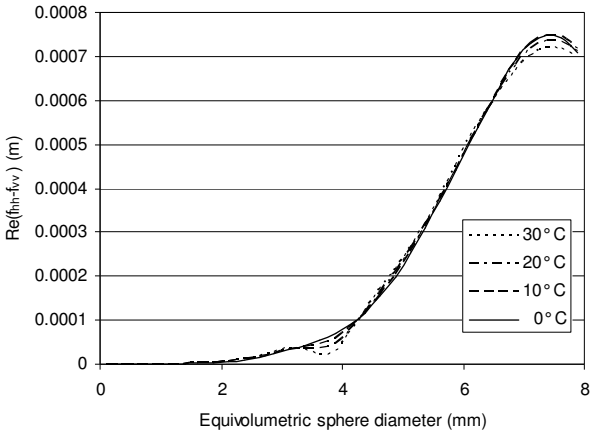

Fig. 5. Difference between the real parts of horizontal and vertical forward scattering amplitude $Re(f_{hh} - f_{vv})$ versus equivolumetric sphere diameter of the raindrop, at 3.1 cm wavelength and temperatures between 0 and 30° C.

6 Effect of raindrop shape models on K_{DP}

In the literature a variety of raindrop shape models exists. It was investigated how different models alter K_{DP} and thus R-K_{DP} relationships for S- and C-band.

Figures 6 and 7 show for S- and C-band the difference between the real parts of horizontal and vertical forward scattering amplitude $Re(f_{hh} - f_{vv})$ versus equivolumetric sphere diameter for several raindrop shape models. The different shape models lead to the R-K_{DP} relationships summarized in Tables 2 and 3.

Table 2. R-K_{DP} relationships determined at S-band for different raindrop-shape models at 10° C

Raindrop shape model	R-K_{DP} relationship
Oguchi (1973)	$R = 41.14\ K_{DP}^{0.959}$
Morrison and Cross (1974)	$R = 37.51\ K_{DP}^{0.959}$
Pruppacher and Beard (1970)	$R = 35.33\ K_{DP}^{0.842}$
Pruppacher and Pitter (1971)	$R = 42.28\ K_{DP}^{0.779}$

Table 3. R-K_{DP} relationships determined at C-band for different raindrop-shape models at 10° C

Raindrop shape model	R-K_{DP} relationship
Oguchi (1973)	$R = 20.24\ K_{DP}^{0.953}$
Morrison and Cross (1974)	$R = 18.46\ K_{DP}^{0.952}$
Pruppacher and Beard (1970)	$R = 18.87\ K_{DP}^{0.835}$
Pruppacher and Pitter (1971)	$R = 23.49\ K_{DP}^{0.773}$

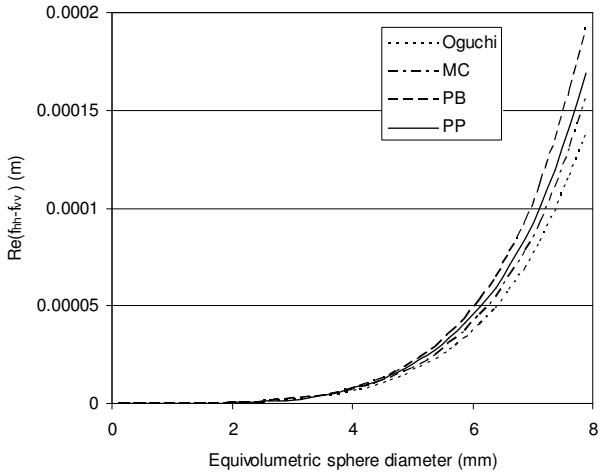

Fig. 6. S-band: Difference between the real parts of horizontal and vertical forward scattering amplitude $Re(f_{hh} - f_{vv})$ versus equivolumetric sphere diameter for several raindrop shape models of Oguchi (1973), Morrison and Cross (MC, 1974), Pruppacher and Beard (PB, 1970), and Pruppacher and Pitter (PP, 1971)

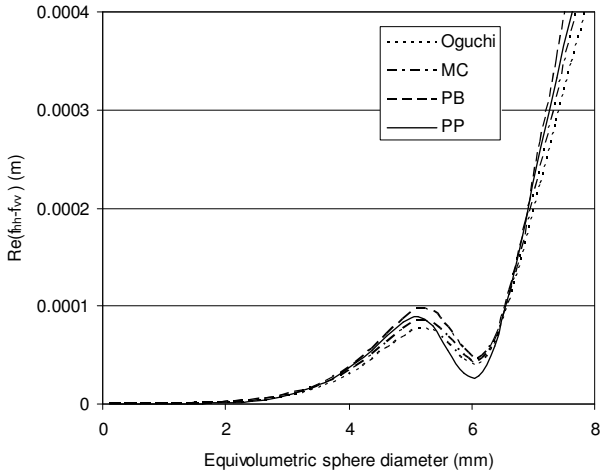

Fig. 7. C-band: Difference between the real parts of horizontal and vertical forward scattering amplitude $Re(f_{hh} - f_{vv})$ over the equivolumetric sphere diameter for several raindrop shape models of Oguchi (1973), Morrison and Cross (MC, 1974), Pruppacher and Beard (PB, 1970), and Pruppacher and Pitter (PP, 1971)

7 Effect of the elevation angle on K_{DP}

The previous simulations were carried out assuming a radar beam parallel to the earth's surface. Below it is observed what effect elevation angles > 0° on the R-K_{DP} relationships have. For these simulations raindrop shapes according Pruppacher and Beard (1970) were assumed.

Tables 4 and 5 give R-K_{DP} relationships for elevation angles up to 30° for S- and C-band.

With increasing elevation angle, K_{DP} decreases, because the raindrop shape seen by the radar becomes more spherical. The decrease of K_{DP} with increasing elevation is shown in Fig. 8. The curve represents an average over all observed

drop-size distributions and is nearly identical at S- and C-band.

Table 4. R-K_{DP} relationships determined at S-band for different elevation angles, at 10° C raindrop temperature.

Elevation angle	R-K_{DP} relationship
0°	$R = 35.33\ K_{DP}^{0.842}$
6°	$R = 35.66\ K_{DP}^{0.842}$
12°	$R = 36.67\ K_{DP}^{0.842}$
18°	$R = 38.45\ K_{DP}^{0.842}$
24°	$R = 41.14\ K_{DP}^{0.842}$
30°	$R = 45.01\ K_{DP}^{0.842}$

Table 5. R-K_{DP} relationships determined at C-band for different elevation angles, at 10° C raindrop temperature.

Elevation angle	R-K_{DP} relationship
0°	$R = 18.87\ K_{DP}^{0.835}$
6°	$R = 19.04\ K_{DP}^{0.835}$
12°	$R = 19.58\ K_{DP}^{0.835}$
18°	$R = 20.52\ K_{DP}^{0.835}$
24°	$R = 21.96\ K_{DP}^{0.835}$
30°	$R = 23.99\ K_{DP}^{0.835}$

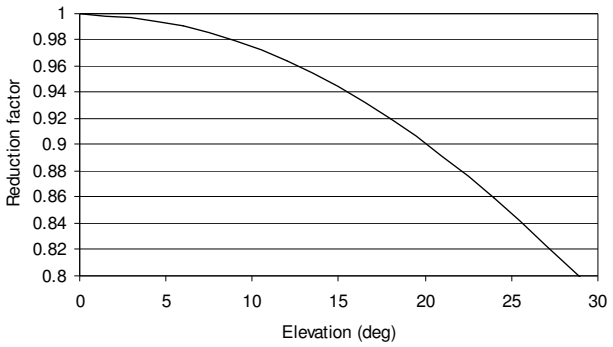

Fig. 8. Reduction factor for K_{DP} with increasing elevation angle for Pruppacher-Beard raindrop shapes at S- and C-band.

8 Effect of raindrop canting

R-K_{DP} relations are slightly affected by canting of raindrops. Aydin and Giridhar (1992) illustrated the effects by using a simple Gaussian canting model with mean value 0° and standard deviation 10°. In their model, canting leads to an underestimation of R by 6%. They conclude, that at C-band the effects of raindrop temperature are more significant than canting.

9 Conclusions

The R-K_{DP} relationships found for S- and C-band (2), (3) are in close agreement with the findings of Aydin and Giridhar (1992). Indeed, a big part of the variation of the relationships in Table 1 is due to different drop-size distributions. But it could be shown, that other raindrop-shape models could alter K_{DP} in the simulation by more than 25 % and therefore can also account for a wide range of R-K_{DP} relationships. The simulations also show that at C-band the raindrop temperature can influence K_{DP} strongly if the radar volume contains a significant number of raindrops > 5 mm. As K_{DP} measurements are noisy, $R(K_{DP})$ estimators are mainly stable at high rainrates with big drop sizes. Especially for such cases the effect of temperature on K_{DP} cannot be neglected.

References

Aydin, K., and V. Giridhar, 1992: C-Band Dual-Polarization Radar Observables in Rain, *J. Atmos. and Oceanic Techn.*, **9**, 383-390.

Bringi, V. N., and V. Chandrasekhar, 2001: *Polarimetric Doppler Weather Radar. Principles and Applications.* Cambridge University Press. 636 pp.

Illingworth, A. J., and T. M. Blackman, 2002: The Need to Represent Raindrop Size Spectra as Normalized Gamma Distributions for the Interpretation of Polarization Radar Observations. *Journal of Applied Meteorology*, **41**, 286-297.

Jameson, A. R., 1991: A Comparison of Microwave Techniques for Measuring Rainfall. *Journal of Applied Meteorology*, **30**, 32-54.

Morrison, J. A., and M. J. Cross, 1974: Scattering of a plane electromagnetic wave by axisymmetric raindrops, *Bell Syst. Tech. J.*, **53**, 955-1019.

Oguchi, T., 1973: Attenuation and phase rotation of radio waves due to rain: Calculations at 19.3 and 34.8 GHz. *Radio Sci.*, **8**, 31-38.

Oguchi, T., 1983: Electromagnetic wave propagation and scattering in rain and other hydrometeors. *Proc. IEEE*, **71**, 1029-1078.

Pruppacher, H. R., and K. V. Beard, 1970: A wind tunnel investigation of the internal circulation and shape of water drops falling at terminal velocity in air. *Quart. J. Roy. Meteor. Soc.*, **96**, 247-256.

Pruppacher, H. R., and R. L. Pitter, 1971: A semi-empirical determination of the shape of cloud and rain drops. *J. Atmos. Sci.,* **28**, 86-94.

Ray, P. S., 1972: Broadband complex refractive indices of ice and water, *Appl. Opt.* **11**, 1836-1844.

Sachidananda, M., and D. S. Zrnić: 1987: Rain rate estimates from differential polarization measurements. *J Atmos. Oceanic Techn.*, **4**, 588-598.

Schönhuber, M., H. Urban, J. P. V. Poiares Baptista, W. L. Randeu and W. Riedler, 1994: Measurements of Precipitation Characteristics by a New Distrometer. Proceedings of *Atmospheric Physics and Dynamics in the Analysis and Prognosis of Precipitation Fields*, November 15 - 18, 1994, Rome, Italy.